# Josephson Directional Amplifier for Quantum Measurement of Superconducting Circuits

Baleegh Abdo,* Katrina Sliwa, S. Shankar, Michael Hatridge, Luigi Frunzio, Robert Schoelkopf, and Michel Devoret†
*Department of Applied Physics, Yale University, New Haven, Connecticut 06520, USA*
(Received 25 November 2013; published 22 April 2014)

We realize a microwave quantum-limited amplifier that is directional and can therefore function without the front circulator needed in many quantum measurements. The amplification takes place in only one direction between the input and output ports. Directionality is achieved by multipump parametric amplification combined with wave interference. We have verified the device noise performances by using it to read out a superconducting qubit and observed quantum jumps. With an improved version of this device, the qubit and preamplifer could be integrated on the same chip.

DOI: 10.1103/PhysRevLett.112.167701 PACS numbers: 84.30.Le, 42.25.Hz, 85.25.Cp

Quantum nondemolition (QND) measurements often require probing a quantum system with a signal containing only a few photons [1]. Measuring such a weak signal with high fidelity in the microwave domain involves a high-gain, low-noise chain of amplifiers. However, state-of-the-art amplifiers, such as those based on high electron mobility transistors (HEMT), are not quantum limited [2]; they add the noise equivalent of about 20 photons at the signal frequency when referred back to the input. They can also have strong in-band and out-of-band backaction on the quantum system. In an attempt to minimize the noise added by the output chain, quantum-limited amplifiers based on parametric processes [3–7] have been recently developed and used as preamplifiers before the HEMT [8–11]. These quantum-limited devices, however, amplify in reflection [3,4,7] and some of them [3,4] have in addition strong reflected pump tones in-band which cause undesirable excess backaction on the quantum system. These devices also do not protect the measured system from backaction originating higher up in the amplification chain. Thus, nonreciprocal devices, such as circulators and isolators, are required in these measurements both to separate input from output and to protect the quantum system from unwanted backaction.

To achieve nonreciprocity, circulators and isolators exploit a magneto-optical effect known as Faraday rotation, which relies on ferrites and permanent magnets, in order to distinguish between polarized waves propagating in opposite directions [12,13]. Despite the reliability and good isolation of these components, utilizing them in low-noise quantum measurements of superconducting circuits has several drawbacks: 1) they are large in size, thus limiting the scalability of quantum systems, 2) their reliance on magnetic materials prevents integration on chip using present technology and makes them incompatible with superconducting circuits, and 3) they add noise to the processed signal as a result of their insertion loss; this loss is particularly critical when they precede the preamplifier.

Hence, the question which we are addressing in this Letter is whether it is possible in principle to build a two-port directional amplifier based on the Josephson effect, which 1) works in the microwave domain (e.g., 4–12 GHz), 2) amplifies in one direction (i.e., nonreciprocal), 3) can amplify both quadratures of the microwave field (i.e., it is phase preserving), 4) adds a minimum amount of noise required by quantum mechanics (i.e., it is quantum limited), 5) is matched to the input and output, 6) has as little in-band and out-of-band excess backaction on quantum systems as possible, where backaction here refers to the excess noise above the quantum noise which the device sends back to its input when amplifying a signal, and 7) has gain, bandwidth, frequency tunability, and dynamic range comparable to existing state-of-the-art parametric amplifiers [7,14].

As we show in this work, the answer to this question is an affirmative yes. Earlier implementations of directional amplifiers have met with difficulties in satisfying all the aforementioned criteria. For example, superconducting quantum interface device (SQUID)-based directional amplifiers, such as the microstrip SQUID amplifier (MSA) [15–17] and the superconducting low-inductance undulatory galvanometer (SLUG) [18,19], dissipate energy on chip and have out-of-band backaction which still requires using circulators in quantum measurements [20]. There is also a different type of directional amplifier known as the traveling-wave parametric amplifier in which the nonlinearity of the kinetic inductance of superconducting transmission lines [21] or Josephson junctions [22] is exploited in order to parametrically amplify weak propagating signals. To the best of our knowledge, the added noise and backaction of this type of amplifier has not yet been fully characterized in a quantum measurement.

The Josephson directional amplifier (JDA) consists of two nominally identical nondegenerate quantum-limited amplifiers, known as the Josephson parametric converter (JPC) [6,7], coupled together through their signal and idler ports [23]. As shown previously, coupling two JPCs

 

together can, under certain conditions, generate directional amplification for a certain applied pump phase difference between the two stages [24]. However, despite the relatively good performances of the proof-of-principle device presented in Ref. [24], it had three main shortcomings: 1) the reflection gain at the desired working point is only suppressed on one port of the device, 2) the added noise and backaction of the device cannot be easily modeled or characterized, and 3) the precise interfering modes which give rise to directional amplification could not be pinned down exactly.

In this Letter, we develop a novel coupling scheme between the two JPCs which meets the requirements for quantum measurements, resolves the problems of the previous design, and leads to a calculable amplifier [23]. The basic idea of the JDA is to transform the nonreciprocal phase of the JPC in the transmission-gain mode, which is set by the phase of the pump drive, into a nonreciprocal amplitude response in the full device, by way of wave interference between different paths. These are formed by coupling two JPCs with the same characteristics together through their signal and idler ports. The signal ports are coupled through a symmetric 50/50 beam splitter (i.e., 90 degree hybrid), while the idler ports are connected together in a feedback loop with adequate attenuation. The beam splitter on the signal ports serves as an interferometer, which splits and combines incoming and outgoing waves, and nulls reflections under certain conditions. The feedback loop on the idler side with the attenuation is essential in order to obtain net gain in the device. As shown in the Supplemental Material [23], directional amplification can be generated between ports 1 (input) and 2 (output) of the device, by operating the two JPCs in amplification mode with the same gain and applying a phase difference of $\pi/2$ between the coherent pump drives feeding the two stages.

To verify that the JDA meets the requirements for quantum measurements, we have coupled our JDA to a superconducting qubit-cavity system without any intermediate circulators, as shown in Fig. 1. The main role of the qubit system is to provide an absolute calibration for the JDA performances. In particular, using this setup we demonstrate the capability of the JDA to perform high-fidelity QND measurements of the qubit state (see Figs. 2 and 3), and also observe quantum jumps between the ground and excited states of the qubit (see Fig. 4).

The cavity-qubit system used in the experiment is an aluminum three-dimensional cavity containing a single junction transmon [25]. The resonance frequency of the cavity when the qubit is in the ground state and the cavity bandwidth are $f_{r,g} = 7.7132$ GHz and $\kappa/2\pi = 3.4$ MHz, respectively. The qubit frequency is $f_{eg} = 4.35181$ GHz and the state-dependent shift of the resonator frequency is $\chi/2\pi = 3.7$ MHz. In the experiment, the read-out tone frequency $f_d = 7.71135$ GHz was set to be at the center between the state-dependent resonances $f_{r,g}$ and $f_{r,e}$, and

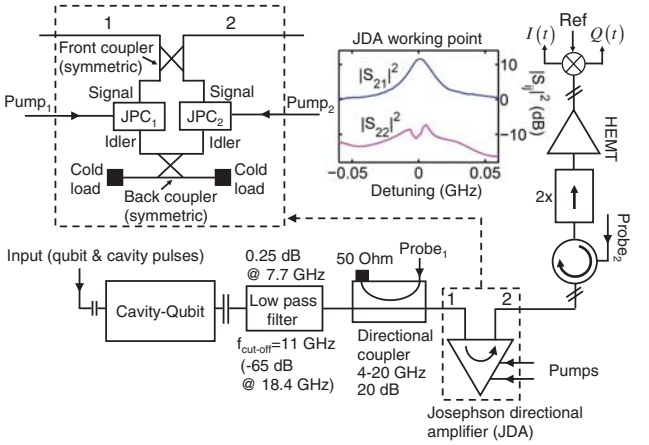


FIG. 1 (color online). Setup used in measuring the performances of the JDA, whose schematic is shown in the inset. A superconducting cavity-qubit system is connected to the input of the JDA with no intermediate circulator or isolator stages. A low-pass filter and a directional coupler are inserted in between the cavity-qubit system and the JDA. The filter protects the cavity-qubit system from high-frequency pump photons that can possibly bounce off the JDA, while the directional coupler enables biasing the JDA at a desired working point using the input Probe$_1$. Similarly, the circulator connected at the output of the JDA enables measuring the reflection off port 2 of the JDA using the input Probe$_2$. The output signal is further amplified using a cryogenic HEMT amplifier and is demodulated at room temperature using a quadrature modulation mixer. The inset displays vector network analyzer measurements of $S_{21}$ and $S_{22}$ of the JDA as a function of frequency detuning relative to the read-out frequency $f_d$, taken at the working point employed in the read-out of the qubit-cavity system.

its power was set to yield an average number of photons in the cavity of 2.9 during the read-out pulse of length $T_m = 250$ ns ($T_m$ is set to 400 ns in the measurements of Figs. 3 and 4).

To read out the qubit state, the center frequency of the JDA was tuned to $f_d$ (the corresponding center frequency on the idler is about 10.75 GHz). This was achieved by varying the flux threading the eight Josephson junction ring modulators of the two JPC stages [7,26]. To operate the JPCs in amplification mode, the frequency of the pump drive feeding them, which is a coherent nonresonant tone, was set to $f_p = 18.464$ GHz, i.e., the sum of the center frequencies of the signal and idler resonators [7]. To improve stability, the pumps applied to both JPCs are generated from a split single generator, with one arm passing through a variable phase shifter and attenuator. The attenuator was inserted in order to compensate for the different amount of attenuation on the pump lines, while the phase shifter was used in order to maximize the directionality of the JDA in the forward direction ($|S_{21}|^2$) for a certain pump amplitude, and at the same time minimize the reflection amplitude on port 2 ($|S_{22}|^2$). Such *in situ* tuning of the JDA working point was enabled by the addition of a

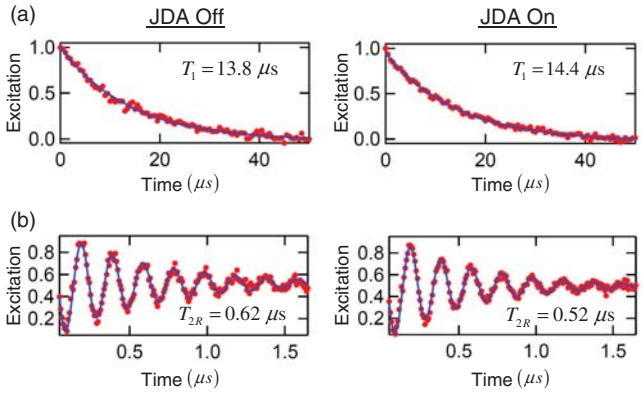


FIG. 2 (color online). A comparison between the decoherence times of the qubit measured with the JDA off (left column) versus on (right column). Plots (a) and (b) show $T_1$ and $T_2$ Ramsey measurement results, respectively. The red filled circles are data points while the blue curves are fits. From the fits we get values for $T_1$ of 13.8 $\mu$s and 14.4 $\mu$s, and values for $T_{2R}$ of 0.62 $\mu$s and 0.52 $\mu$s for the JDA-off versus -on cases, respectively.

directional coupler at the input of the JDA and a circulator at its output, as can be seen in Fig. 1. In addition, a low-pass filter with a cutoff at 11 GHz was added between the cavity and the JDA mainly as a protection for the cavity-qubit system from pump photons that can bounce off the JDA due to the finite isolation (20 dB) between the $\Sigma$ and $\Delta$ ports of the 180 degree hybrids used for feeding the pumps to the JDA (see Fig. S6 in the Supplemental Material [23]). The working point of the JDA at which the data in Figs. 2, 3, and 4 were taken is shown in the inset of Fig. 1. The forward gain of the device is set to $11.6 \pm 1$ dB with a dynamical bandwidth of 15 MHz [23]. It is important to note that the qubit-cavity can also be measured with the JDA pump off. This is because the JDA has a unity transmission in that case [23].

In Fig. 2, we show the relaxation time $T_1$ and $T_{2R}$ of the qubit measured with the JDA off versus on. As can be seen in the figure, turning the JDA on improves the measurement signal-to-noise ratio without any observed degradation in the relaxation time of the qubit or considerable effect on $T_{2R}$. The fact that the JDA does not alter $T_1$ provides an important piece of evidence that it can perform QND measurements. The relatively short $T_{2R} \simeq 0.6$ $\mu$s in both cases can be attributed to the relatively high base temperature of the dilution fridge in the experiment, 54 mK, as well as the relatively short inverse residence rate of photons in the cavity, $1/\kappa = 47$ ns. Knowing $\kappa$ and $T_{2R}$, we can calculate the maximum average number of thermal photons in the cavity required in order to account for the measured $T_{2R}$, which is given by $1/\kappa T_{2R} = 0.08$. Similarly, by subtracting the ratio $1/\kappa T_{2R}$ for the JDA-on versus -off cases, we can set a bound of about 0.01 added photons in the cavity due to the backaction of the JDA. Such a backaction effect can be due to either a pump power of about -150 dBm that leaks back from the JDA and populates a higher resonance mode of the cavity or to low-gain amplified quantum noise which is transmitted in the opposite direction ($S_{12}$) at resonance.

To further verify that the JDA performs a QND operation, we have measured the qubit population in the ground ($p_g$) and excited ($p_e$) states with the JDA on versus off using the measurement method presented in Ref. [27]. In both measurements, we obtained the same nominal result, $p_g = 0.8 \pm 0.02$ and $p_e = 0.2 \pm 0.02$, which shows that

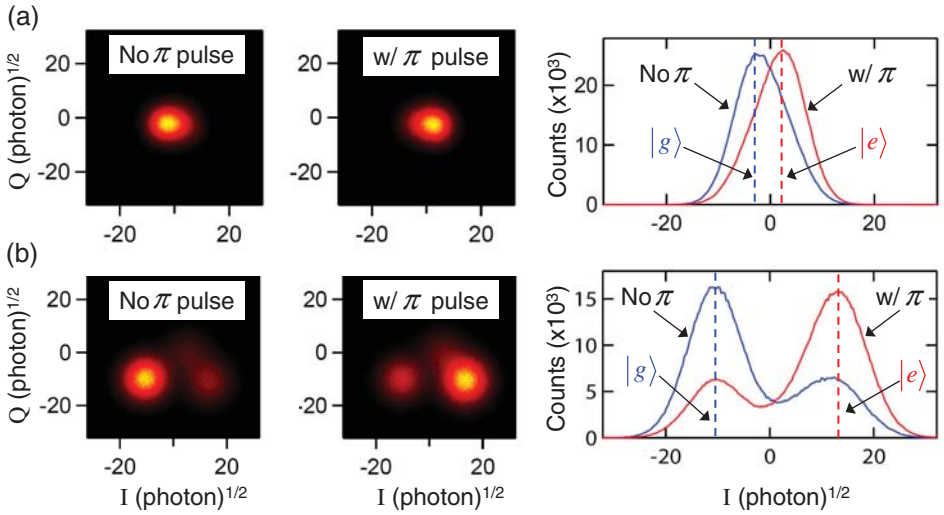


FIG. 3 (color online). Histograms of the qubit state measured after applying a $\pi$ pulse or no pulse to the qubit. Panels (a) and (b) show the histograms measured with the JDA off and on, respectively. In the left and middle columns, we depict two-dimensional histograms of the qubit state as a function of the $I$ and $Q$ quadratures of the microwave field, expressed in units of the square root of the average number of photons in the read-out pulse at the output of the JDA. The right column depicts projections of the two-dimensional histograms for the ground and excited states onto the $I$ quadrature.

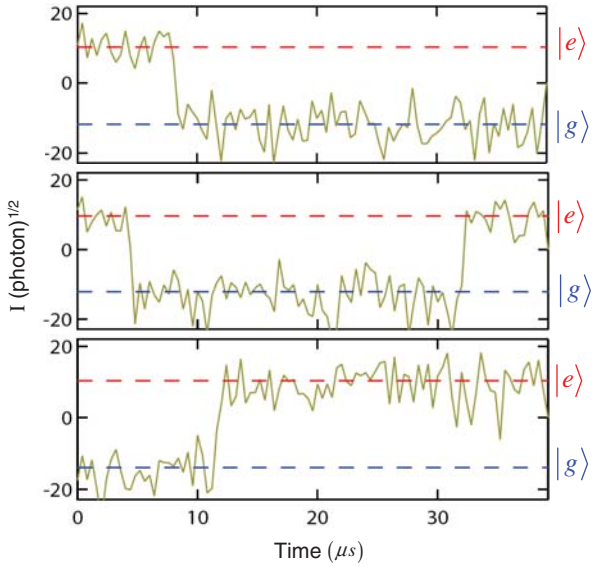


FIG. 4 (color online). Selected individual measurement records of the JDA-on output. The qubit state traces versus time exhibit quantum jumps between the ground and excited states of the qubit. The red and blue dashed lines—which indicate the excited and ground signal levels of the qubit, respectively—are guides for the eye.

the JDA does not affect the qubit population. Furthermore, from these measurements we extract a qubit temperature of $T = 154 \pm 4$ mK.

On the left side of Fig. 3, we depict two-dimensional histograms of single-shot measurements of the qubit state obtained upon applying a $\pi$ pulse or no pulse to the qubit. In Figs. 3(a) and 3(b) we plot the histograms measured with the JDA off and on, respectively, in both quadratures of the microwave field, i.e., $I$ and $Q$, expressed in units of the square root of the average number of photons in the read-out pulse at the output of the JDA. As expected, without applying a pulse (left column) and following a $\pi$ pulse (middle column), the majority of the qubit population is in the ground and excited state, respectively. The main differences between the histograms shown in Fig. 3(b) compared to Fig. 3(a) are that the histograms in Fig. 3(b) are broader and more separated, and a small population in the $f$ state is visible close to the origin, while it is hidden in Fig. 3(a). In the right column, we plot projections of the histograms corresponding to the ground and excited states onto the $I$ quadrature axis. As can be seen in the bottom plot, with the JDA on, the Gaussian curves corresponding to the $g$ and $e$ states are sufficiently separated (about $3.7\sigma$) which allows us to perform single-shot measurements of the qubit state. Moreover, from the standard deviations of the measured histograms for the JDA-off ($\sigma_{\mathrm{Off}}$) and -on ($\sigma_{\mathrm{On}}$) cases, we find that the number of noise photons added by the output chain (with the JDA off) and by the JDA at the signal frequency when referring back to the input are $n_{\mathrm{sys}} = 17 \pm 1$ and $n_{\mathrm{JDA}} = 0.9 \pm 0.4$, respectively. The result for $n_{\mathrm{sys}}$ agrees well with our prior knowledge of the noise temperature of the output line, which is $6.5 \pm 1$ K. Also, as predicted by theory [23], $n_{\mathrm{JDA}}$ shows that the JDA indeed operates near the quantum limit, which is $n = 1/2$ for phase-preserving amplification [2].

In addition, we measured two-dimensional histograms of the qubit state for different drive powers. This allowed us to determine the onset of input power at which the JDA starts to saturate as the histogram separation stops scaling as the square root of the input power. Using this method, we find that this power is about 7 photons at the read-out frequency per inverse cavity bandwidth. This figure of merit can be improved by enhancing the dynamic range of the JPC stages that form the JDA [7].

In Fig. 4 we display three selected individual measurement records of the qubit state. The data are digitized with a sampling time of 20 ns and smoothed with a boxcar filter with 400 ns width, which corresponds to 8.5 cavity lifetimes. As can be seen in the figure, the traces of the qubit state versus time exhibit quantum jumps between the $g$ and $e$ states. It also shows that with the JDA we can perform single-shot measurements of the qubit state and track its state in real time, which are essential requirements for many quantum feedback applications [28,29].

It is important to point out that the JDA gain attained in this experiment is mainly limited by nonidealities in the cavity-qubit setup, such as using infrared filters on the pump lines which are not well matched to 50 ohm [23]. Fixing these problems should allow the JDA to operate at gains in excess of 20 dB. Other potential improvements to the present JDA setup (see the Supplemental Material [23] for a diagram of the JDA implementation) include 1) substituting the commercial hybrids with superconducting on-chip versions [30], which have less insertion loss, smaller phase and amplitude imbalance between the different arms, and larger isolation between the sum and difference ports in the case of the 180 degree hybrids, which are part of the JPC circuit [6,23], 2) substituting the normal coax cable connecting the two idler feedlines with a superconducting transmission line, and 3) implementing all components on the same chip.

In conclusion, we have realized a novel Josephson directional amplifier suitable for quantum measurements and demonstrated its performances by reading out the quantum state of a superconducting qubit. Looking forward, an on-chip version of the directional amplifier presented in this work can be in principle implemented using standard microwave technology and fabrication processes. Moreover, the ability to perform high-fidelity QND measurements without incorporating intermediate circulator stages between the qubit and the quantum-limited amplifier opens the door for realizing quantum systems with high measurement efficiency, in which qubits and preamplifiers are integrated on the same chip.

Discussions with Anirudh Narla are gratefully acknowledged. This research was supported by the NSF under grants DMR-1006060 and DMR-0653377, ECCS-1068642, the NSA through ARO Grant No. W911NF-09-1-0514, and the IARPA under ARO Contract No. W911NF-09-1-0369.

*Present address: IBM T. J. Watson Research Center, Yorktown Heights, New York 10598, USA.
†michel.devoret@yale.edu

[1] C. C. Clerk, M. H. Devoret, S. M. Girvin, F. Marquardt, and R. J. Schoelkopf, Rev. Mod. Phys. **82**, 1155 (2010).
[2] C. M. Caves, Phys. Rev. D **26**, 1817 (1982).
[3] R. Vijay, M. H. Devoret, and I. Siddiqi, Rev. Sci. Instrum. **80**, 111101 (2009).
[4] M. A. Castellanos-Beltran, K. D. Irwin, G. C. Hilton, L. R. Vale, and K. W. Lehnert, Nat. Phys. **4**, 929 (2008).
[5] T. Yamamoto, K. Inomata, M. Watanabe, K. Matsuba, T. Miyazaki, W. D. Oliver, Y. Nakamura, and J. S. Tsai, Appl. Phys. Lett. **93**, 042510 (2008).
[6] B. Abdo, F. Schackert, M. Hatridge, C. Rigetti, and M. Devoret, Appl. Phys. Lett. **99**, 162506 (2011).
[7] B. Abdo, A. Kamal, and M. H. Devoret, Phys. Rev. B **87**, 014508 (2013).
[8] R. Vijay, D. H. Slichter, and I. Siddiqi, Phys. Rev. Lett. **106**, 110502 (2011).
[9] D. Ristè, J. G. vanLeeuwen, H.-S. Ku, K. W. Lehnert, and L. DiCarlo, Phys. Rev. Lett. **109**, 050507 (2012).
[10] Z. R. Lin, K. Inomata, W. D. Oliver, K. Koshino, Y. Nakamura, J. S. Tsai, and T. Yamamoto, Appl. Phys. Lett. **103**, 132602 (2013).
[11] M. Hatridge *et al.*, Science **339**, 178 (2013).
[12] D. M. Pozar, *Microwave Engineering*, 3rd ed., (Wiley, Hoboken, NJ, 2005).
[13] A. Kamal, Ph. D. Thesis, Yale University, 2013.
[14] M. Hatridge, R. Vijay, D. H. Slichter, J. Clarke, and I. Siddiqi, Phys. Rev. B **83**, 134501 (2011).
[15] L. Spietz, K. Irwin, and J. Aumentado, Appl. Phys. Lett. **93**, 082506 (2008).
[16] M. Mück, D. Hover, S. Sendelbach, and R. McDermott, Appl. Phys. Lett. **94**, 132509 (2009).
[17] D. Kinion and J. Clarke, Appl. Phys. Lett. **98**, 202503 (2011).
[18] G. J. Ribeill, D. Hover, Y.-F. Chen, S. Zhu, and R. McDermott, J. Appl. Phys. **110**, 103901 (2011).
[19] D. Hover, Y.-F. Chen, G. J. Ribeill, S. Zhu, S. Sendelbach, and R. McDermott, Appl. Phys. Lett. **100**, 063503 (2012).
[20] J. E. Johnson, E. M. Hoskinson, C. Macklin, D. H. Slichter, I. Siddiqi, and J. Clarke, Phys. Rev. B **84**, 220503 (2011).
[21] B. H. Eom, P. K. Day, H. G. LeDuc, and J. Zmuidzinas, Nat. Phys. **8**, 623 (2012).
[22] O. Yaakobi, L. Friedland, C. Macklin, and I. Siddiqi, Phys. Rev. B **87**, 144301 (2013).
[23] See Supplemental Material at http://link.aps.org/supplemental/10.1103/PhysRevLett.112.167701 for a generic scheme of the JDA, a calculation of the general scattering matrix of the JDA, a discussion of the JDA performances, a circuit diagram of the JDA used in the experiment, possible improvements to the JDA circuit, and a measured working point of the JDA.
[24] B. Abdo, K. Sliwa, L. Frunzio, and M. H. Devoret, Phys. Rev. X **3**, 031001 (2013).
[25] H. Paik *et al.*, Phys. Rev. Lett. **107**, 240501 (2011).
[26] N. Roch, E. Flurin, F. Nguyen, P. Morfin, P. Campagne-Ibarcq, M. H. Devoret, and B. Huard, Phys. Rev. Lett. **108**, 147701 (2012).
[27] K. Geerlings, Z. Leghtas, I. Pop, S. Shankar, L. Frunzio, R. Schoelkopf, M. Mirrahimi, and M. Devoret, Phys. Rev. Lett. **110**, 120501 (2013).
[28] R. Vijay, C. Macklin, D. H. Slichter, S. J. Weber, K. W. Murch, R. Naik, A. N. Korotkov, and I. Siddiqi, Nature (London) **490**, 77 (2012).
[29] D. Ristè, *et al.*, Nature (London) **502**, 350 (2013).
[30] H. S. Ku, F. Mallet, L. R. Vale, K. D. Irwin, S. E. Russek, G. C. Hilton, and K. W. Lehnert, IEEE Trans. Appl. Supercond. **21**, 452 (2011).